

Electrochemical Reduction of Aqueous Imidazolium on Pt(111) by Proton Coupled Electron Transfer

Kuo Liao · Mikhail Askerka · Elizabeth L. Zeitler ·
Andrew B. Bocarsly · Victor S. Batista

Published online: 21 November 2014
© Springer Science+Business Media New York 2014

Abstract Recent electrochemical studies have reported aqueous CO₂ reduction to formic acid, formaldehyde and methanol at potentials of ca. –600 mV versus SCE, when using a Pt working electrode in acidic pyridine solutions. In those experiments, pyridinium is thought to function as a one-electron shuttle for the underlying multielectron reduction of CO₂. DFT studies proposed that the critical step of the underlying reaction mechanism is the one-electron reduction of pyridinium at the Pt surface through proton coupled electron transfer. Such reaction forms a H adsorbate that is subsequently transferred to CO₂ as a hydride, through a proton coupled hydride transfer mechanism where pyridinium functions as a Brønsted acid. Here, we find that imidazolium exhibits an electrochemical behavior analogous to pyridinium, as characterized by the experimental and theoretical analysis of the initial reduction on Pt. A cathodic wave, with a cyclic voltammetric half wave potential of ca. –680 mV versus SCE, is consistent with the theoretical prediction based on the recently proposed reaction mechanism suggesting that positively charged Brønsted acids could serve as electrocatalytic one-electron shuttle species for multielectron CO₂ reduction.

Keywords Imidazolium · DFT · CO₂ reduction ·
Electrocatalysis · PCET

K. Liao · E. L. Zeitler · A. B. Bocarsly (✉)
Department of Chemistry, Princeton University, Princeton,
NJ 08544, USA
e-mail: bocarsly@princeton.edu

M. Askerka · V. S. Batista (✉)
Department of Chemistry, Yale University,
P.O. Box 208107, New Haven, CT 06520, USA
e-mail: victor.batista@yale.edu

1 Introduction

The electrocatalytic reduction of carbon dioxide (CO₂) at low overpotentials is a process of great current interest since it could provide a viable solution to the generation of fuels with a carbon neutral atmospheric footprint [1–3]. Recent studies have reported CO₂ reduction to formic acid, formaldehyde and methanol at low overpotentials of ca. –600 mV versus SCE, when using a Pt disk electrode and a 10 mM aqueous solutions of pyridine (Pyr) at pH 5.3 (Fig. 1) [4].

The underlying reaction mechanism has yet to be established, however, several mechanisms have been proposed. The first mechanistic proposal suggested a globally homogeneous process based on inner-sphere-type electron transfer from the pyridinium radical (PyrH[•]) to the substrate (Fig. 2) [4]. Such a mechanism requires the generation of the PyrH[•] intermediate according to the one-electron reduction of the pyridinium cation (PyrH⁺) (Fig. 2, ii) and formation of a carbamate intermediate (Fig. 2, iii) [5]. Reduction of the carbamate by reaction with another PyrH[•] produces formic acid (Fig. 2, iv). Formic acid could react analogously to form formaldehyde, and then formaldehyde could get reduced analogously to form methanol. This proposal was supported by simulations of the cyclic voltammetric scan rate dependence on a Pt electrode, by the first order dependence of current on concentrations of both PyrH⁺ and CO₂, and by some density functional theory (DFT) calculations [4–6]. In addition, the carbamate C–N stretching mode was probed by gas-phase vibrational spectroscopy of Pyr embedded in CO₂ clusters [7]. Reduction of CO₂ to methanol in the presence of PyrH⁺ has also been observed photochemically, suggesting that reduction of PyrH⁺ may be possible in the homogeneous phase when using a photocatalyst with sufficiently negative redox potential [8], as indicated by

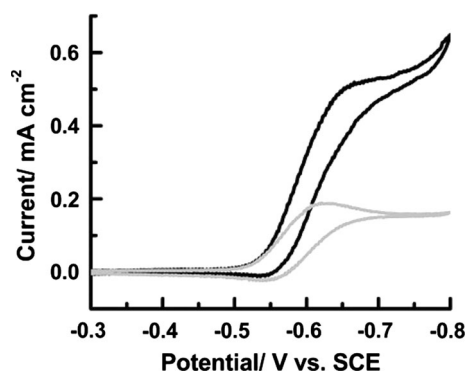


Fig. 1 Cyclic voltammograms of PyrH^+ reduction in the presence of Ar (gray) and CO_2 (black) at pH = 5.3, obtained with a Pt disk electrode [1]. Figure reproduced from reference 1 with permission. Copyright American Chemical Society 2010

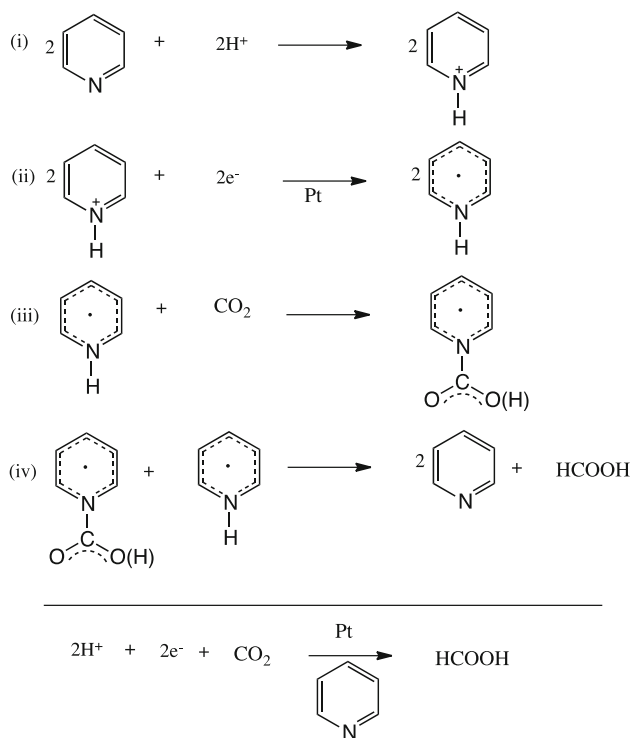


Fig. 2 Proposed CO_2 reduction mechanism based on homogeneous reduction of PyrH^+ to PyrH^\bullet (ii), followed by formation of the carbamate intermediate (iii) and inner-sphere-type electron transfer from the pyridinium radical to the substrate (iv)

quenching measurements [9]. However, to date, there has been no direct observation of the pyridinium radical or carbamate intermediates under working electrochemical conditions. In addition, DFT studies have ruled out the possibility of homogeneous reduction of PyrH^+ to PyrH^\bullet at low overpotentials [10, 11], since the calculations suggested that a significantly more negative reduction potential than -600 mV versus SCE is necessary to reduce PyrH^+ to PyrH^\bullet in solutions. Some of these DFT studies suggested other mechanistic pathways for the initial

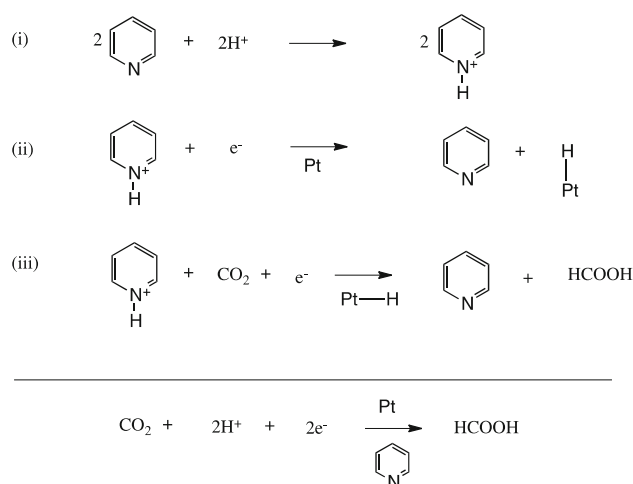


Fig. 3 Proposed mechanism of electrochemical reduction of CO_2 on Pt(111), in aqueous acidic pyridine solution, based on DFT calculations at PBE level of theory

reduction of PyrH^+ including two electron reduction of PyrH^+ to dihydropyridine [11], assisted deprotonation of pyridinyl via a hydrogen bound intermediate [12], and specific adsorption of PyrH^+ or pyridinyl [10, 12]. However, these proposals were not supported by experimental studies of CO_2 reduction on Pt electrodes [9].

An alternative mechanism proposed by another DFT study [13] involves reduction of PyrH^+ to hydrogen (Fig. 3, ii) by proton coupled electron transfer (PCET), as the electrochemical step responsible for the cathodic wave of ca. -600 mV versus SCE, when using a Pt disk electrode in a 10 mM aqueous solution of Pyr at pH 5.3. The hydrogen adsorbates are susceptible to electrophilic attack by CO_2 when activated by hydrogen bonding with PyrH^+ (Fig. 3, iii), and are transferred as hydrides to CO_2 according to an effective proton-coupled-hydride-transfer (PCHT) reaction. The mechanism involves a one-electron rate limiting step on the electrode surface (step ii, Fig. 3) and therefore accounts for the observation of a quasireversible one-electron cathodic wave (Fig. 1, black line). It also accounts for the sensitivity of the reaction to the nature of the working electrode, with significant activity for metal surfaces that adsorb hydrogen (such as Pt) but no catalytic current for glassy carbon electrodes at low overpotentials. According to such a mechanism, PyrH^+ is an electrocatalytic Brønsted acid, with $\text{p}K_a^{\text{PyrH}^+} = 5.17$ that establishes an effective concentration of positively charged acid $[\text{PyrH}^+] = 4.26$ mM in contact with the negatively charged Pt surface, much higher than the concentration of protons in solution ($[\text{H}^+] = 5 \times 10^{-3}$ mM). Therefore, it is natural to expect that other positively charged Brønsted acids, such as imidazolium, would interact with the negatively charged Pt surface analogously and exhibit a similar electrocatalytic behavior.

The proposed reduction of the Brønsted acid PyrH^+ on a metallic (Pt) electrode that adsorbs hydrogen is consistent with earlier studies [14]. Such a mechanism is also supported by the observed dependence on $\text{p}K_a$ of the redox potentials of various acids reduced on Pt [9, 15], and with several studies of reductive adsorption of hydrogen on Pt electrodes investigated by cyclic voltammetry (CV) [16], sum frequency generation IR spectroscopy [17], and surface enhanced Raman spectroscopy [18]. Furthermore, several papers have reported under potential deposition of a monolayer of adsorbed hydrogen on Pt surfaces [19–24], including adsorption to the three fold fcc sites of Pt(111) [25, 26], and submonolayer deposition of more weakly adsorbed hydrogen atoms on-top of Pt at the hydrogen redox potential [27].

In a recent electrochemical study that will be published elsewhere we have found further evidence supporting PyrH^+ reduction to hydrogen, including both equilibrium and kinetic isotopic effects on the underlying reduction upon substitution of the acidic hydrogen of PyrH^+ by deuterium. These observations included a shift in the potential of the cathodic wave by -25 mV when comparing PyrD^+ in D_2O to PyrH^+ in H_2O , and a KIE of ~ 1.4 for PyrH^+ reduction. Deuteration changes the zero point energy (ZPE) of the NH bond and therefore the molecular entropy of the Brønsted acid [28], stabilizing the deuterated species from reductive deprotonation. The observed equilibrium isotope effect (EIE) is therefore consistent with N–H bond breaking during PyrH^+ reduction by PCET.

Considering the current level of support of the proposed reaction mechanism based on reduction of the positively charged Brønsted acid PyrH^+ to hydrogen adsorbed on the metal electrode and Pyr in solution, it is important to analyze whether other Brønsted acids (e.g., imidazolium) exhibit analogous electrochemical behavior under similar experimental conditions of concentration, pH and working electrode as explored in this paper. Our analysis suggests that positively charged Brønsted acids, such as imidazolium and pyridinium, can be reduced at low overpotentials. These results also support the mechanistic hypothesis that formation of surface hydride might allow for electrochemical reduction of CO_2 on metallic electrodes at low overpotentials as shown in Fig. 2 through the PCHT reaction pathway that avoids formation of high energy intermediates as in homogeneous catalysis [2, 29, 30].

2 Methods

2.1 DFT Calculations

DFT calculations were performed at the gradient-corrected PBE level [31] within the plane-wave pseudopotential

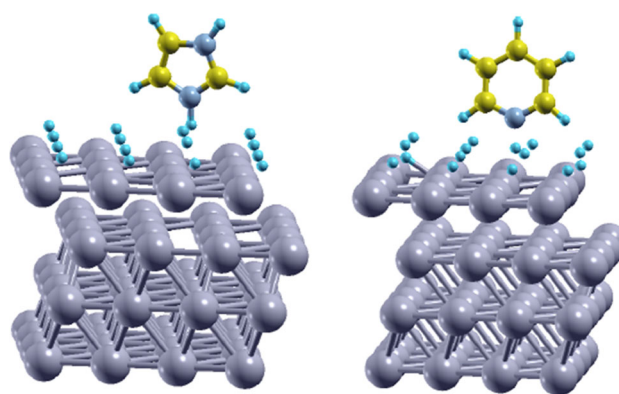


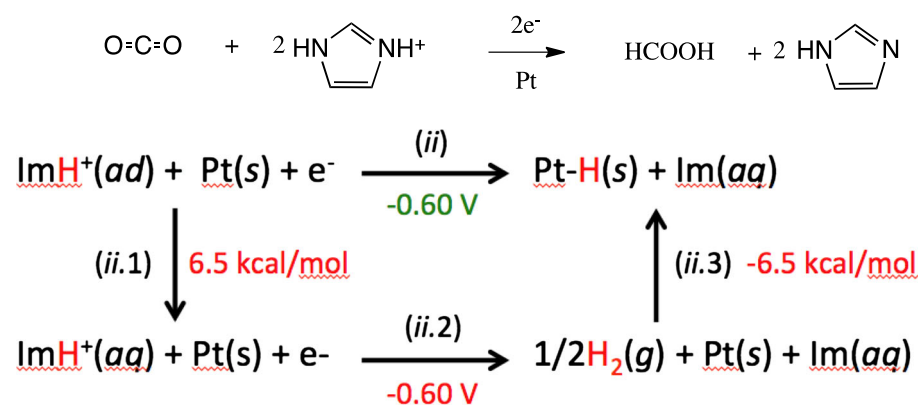
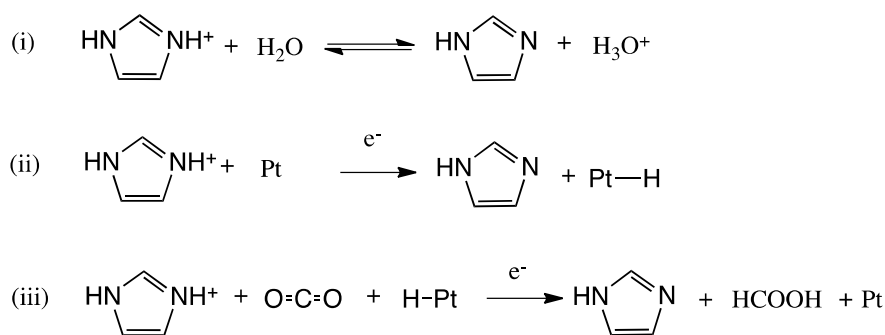
Fig. 4 DFT model structures of imidazolium (*left*) and pyridinium (*right*) on a Pt(111) surface covered with hydrogen adsorbates built by periodically repeating a 3×3 supercell ($8.49 \times 8.49 \text{ \AA}^2$) in a four-layer slab

scheme implemented in Quantum ESPRESSO [32]. Ultra-soft pseudopotentials for Pt, C, H and N atoms were employed with cut off plane wave kinetic energies of 40 Ry for the wavefunctions and 480 Ry for the charge densities. The Pt(111) surface was modeled by a periodically repeating 3×3 supercell ($8.49 \times 8.49 \text{ \AA}^2$) in a four-layer slab (Fig. 4). The two bottom layers were fixed at the bulk lattice geometry. The Pt(111) surface is covered with a monolayer of hydrogen ad-atoms, adsorbed to the fcc sites. The Monkhorst–Pack type of k-point sampling with a $2 \times 2 \times 1$ grid was chosen for the slab calculations.

Thermodynamic data for free energy computations were obtained from structural model clusters fully optimized at the PBE level of DFT [31], using the Stuttgart RSC 1997 ECP basis set (SDD) [33] for Pt, and the 6-31G(d) basis set [34] for C, H and N, as implemented in Gaussian 09 [35]. The reduction potential of ImH^+ to H_2 and imidazole was calculated using a larger 6-311 + G(2df,p) basis set. Thermal contributions to molecular free energies included the ideal-gas, rigid-rotator, and harmonic oscillator approximations [36]. Solvation effects were accounted for by using the SMD aqueous continuum solvation model [37]. The solvation contribution to the plane-wave-based periodic DFT optimized structures were estimated by using model clusters with 14 Pt atoms and performing calculations at the PBE/DFT level, using the SDD basis set for Pt and the 6-31G(d) basis set for all other atoms while restricting the spin state of model structures to open-shell singlet, or doublet states.

Free energy changes due to reduction of ImH^+ on Pt(111) were computed by using the thermodynamic cycle shown in Fig. 5 (bottom panel). The cycle includes surface desorption of ImH^+ (ii.1), reduction of ImH^+ to H_2 and imidazole, in the aqueous solution (ii.2), and dissociative

Fig. 5 *Top* Proposed mechanism of electrochemical reduction of CO₂ on Pt(111) in an aqueous imidazole solution (pH = 5.2). *Bottom* Thermodynamic cycle (ii.1)–(ii.3) used to obtain the free energy change due to reduction of ImH⁺ adsorbed to the Pt surface to form Pt-hydride on the surface



adsorption of H₂ to the Pt surface (ii.3). The reduction potential of ImH⁺ to H₂ and imidazole (ii.2) was predicted to be −0.60 V, in good agreement with the reduction potential observed by CV experiments, while the free energy changes for reactions (ii.1) and (ii.3) approximately cancel each other.

The free energy change associated with the dissociative adsorption of H₂ to the Pt surface (ii.3) was −6.5 kcal/mol, consisting of the sum of ΔE = −8.2 kcal/mol (via plane-wave-based periodic DFT calculations), plus ZPE (−3.1 kcal/mol) and entropy (3.9 kcal/mol) contributions and solvation contributions of +0.8 kcal/mol (via cluster calculations). The free energy change for desorption of ImH⁺ (ii.1) was ΔG^{desorp} = 6.5 kcal/mol which consisted of ΔE = 76.1 kcal/mol, ΔZPE = + 6.5, entropic contribution of −TΔS = −6.0 kcal/mol and solvation ΔG^{solv} = −70.1 kcal/mol. The free energy sum of (ii.1)–(ii.3) yields a calculated reduction potential for (ii) of −0.60 V. For comparison, Fig. 6 shows that the reduction of imidazolium and pyridinium in aqueous solutions to the corresponding imidazolium and pyridinium radicals occur at much more negative potentials than observed in the cyclic voltammogram measurements.

2.2 Electrochemical Experiments

The electrochemical experiments were carried out using a three-electrode cell, with a mesh Pt counter electrode, and a saturated calomel electrode (SCE) as reference (with a potential of +0.241 V versus the standard hydrogen electrode (SHE) at 25 °C). The working electrodes were BASi Pt disk electrodes 0.16 cm in diameter. The electrolyte solution was 0.5 M KCl_{aq} (Sigma-Aldrich). Cyclic voltammograms were recorded on either CHI 760 or CHI 1140 potentiostats. Between each scan, the working electrode was polished with 1 μm alumina (Fisher) supported on a cloth pad. Argon was used to purge the solution and electrochemical cell ensuring an inert gas atmosphere. The solution pH was adjusted by using hydrochloric acid and potassium hydroxide solutions, and monitored by using a pH meter (Denver Instrument). Aqueous cyclic amine solutions were prepared at 10 mM concentrations.

2.3 Results and Discussion

Figure 7 compares the cyclic voltammograms of imidazolium ImH⁺ (black) and pyridinium PyH⁺ (red) reduction

Fig. 6 Calculated potentials for reduction of aqueous pyridinium (*left*) and imidazolium (*right*) to form the 1-electron radical (*red, top*) or H₂ evolution (*blue bottom*), as compared to the observed experimental mid-point potentials (*green*) obtained from Fig. 7 and Table 1

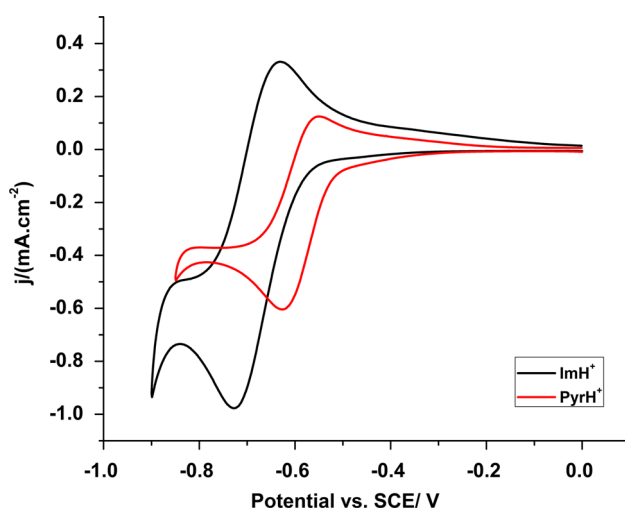
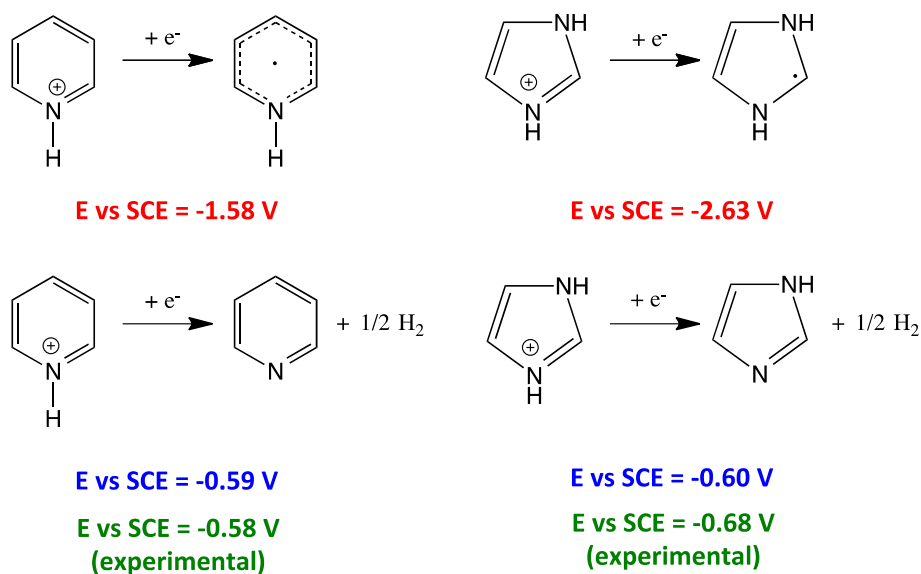


Fig. 7 Cyclic voltammograms at 10 mV/s scan rate at a Pt electrode with an electrolyte containing 10 mM imidazolium (*black*) and pyridinium (*red*) individually. Solutions were pre-purged with Ar and the pH was adjusted to 5.2. The supporting electrolyte was 0.5 M KCl

on a Pt electrode, as recorded at a scan rate of 10 mV/s. The detailed readings for the peak current potentials, half-wave potentials ($E_{1/2}$) and onset potentials, from Fig. 7, are reported in Table 1. These results show that the reduction of aqueous imidazolium is very similar to the reduction of pyridinium with $E_{1/2}(\text{ImH}^+) = -0.68$ V versus SCE which is shifted by only 100 mV when compared to pyridinium with a cathodic wave at $E_{1/2}(\text{PyrH}^+) = -0.58$ V versus SCE. The onset and peak current potentials are also very similar, as shown in Table 1, consistent with a common reduction mechanism.

The values of $E_{1/2}$ are found to be independent of the concentration of the redox species, with average values for

Table 1 Potentials (in Volts vs. SCE) for the peak current, half-wave potentials and onset potentials from the cyclic voltammograms shown in Fig. 7

	Peak	$E_{1/2}$	Onset
ImH ⁺	-0.72	-0.68	-0.56
PyrH ⁺	-0.62	-0.58	-0.51

ImH⁺ and PyrH⁺ of -0.68 and -0.58 V versus SCE, respectively. These half-wave potentials are related to the formal redox potentials ($E^{o'}$) by $\ln(\frac{D_R}{D_O})$ where D_R and D_O are the diffusion coefficients for the reduced and oxidized species [38]. As shown in the Fig. 8, the $E_{1/2}$ values are independent of the scan rate over the explored range of 10–5,000 mV/s, indicating that the diffusion logarithmic term is well approximated as zero for both amines. Therefore, the approximation $E_{1/2} = E^{o'}$ is valid.

The proposed reduction mechanism is an inner-sphere acid-bound proton reduction to surface hydride that implies a linear relationship between the formal redox potentials $E_{\text{HA}/\text{H}(\text{Pt})\text{A}^-}^{o'}$ and the $\text{p}K_a$ of the Brønsted acid (HA), with a slope of -59 mV per unit of $\text{p}K_a$ as predicted from the Nernst equation (see Appendix): $E_{\text{HA}/\text{H}(\text{Pt})\text{A}^-}^{o'} = E_{\text{H}^+/\text{H}(\text{Pt})}^{o'} - 59 \text{mV } \text{p}K_{a(\text{HA})}$, where $E_{\text{H}^+/\text{H}(\text{Pt})}^{o'}$ is the formal redox potential of H⁺ on Pt. The predicted linear relationship is consistent with the observed redox potentials since the $\text{p}K_a$ s of ImH⁺ and PyrH⁺ are 7.1 and 5.17, respectively, predicting formal redox potentials -663 and -549 mV versus SCE for reduction of ImH⁺ and PyrH⁺, respectively, in very good agreement with the observed mid-point potentials of -680 and -580 mV versus SCE (Table 1), and the corresponding shift of -100 mV when comparing

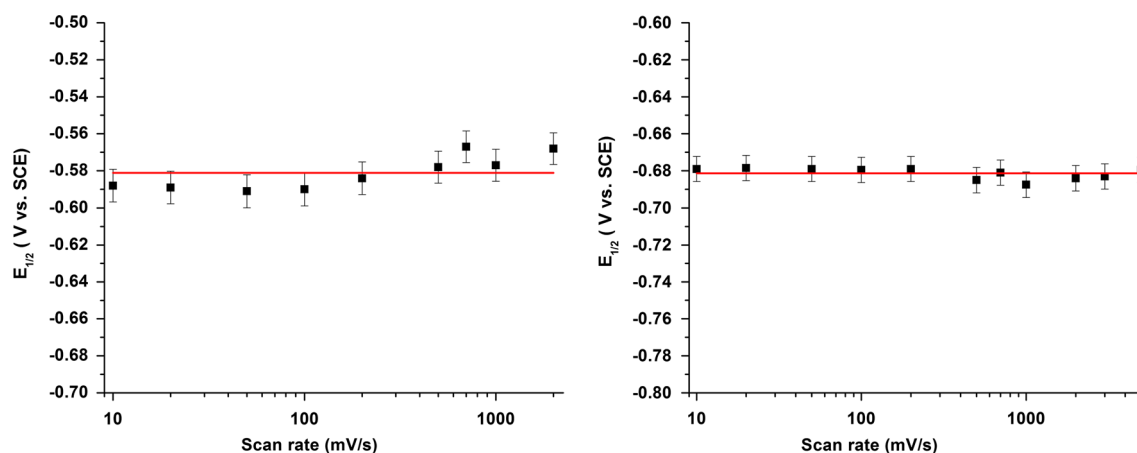


Fig. 8 $E_{1/2}$ potentials versus log scale of scan rates for pyridinium (*left*) and imidazolium (*right*) reductions on Pt electrode. Both Brønsted acids show good linearity with average mid-point potentials of -0.58 and -0.68 V versus SCE for pyridinium and imidazolium, respectively

the reduction of ImH^+ to that of PyrH^+ . These results thus show that imidazolium exhibits an electrochemical behavior analogous to pyridinium, ascribed to a reduction mechanism that forms a surface hydride on the Pt electrode.

3 Conclusions

We have found that imidazolium exhibits an electrochemical behavior analogous to pyridinium, with a mid-wave potential of -680 mV versus SCE for the one-electron reductive cathodic wave of cyclic voltammogram measurements. The theoretical analysis suggests that imidazolium must share a common reduction mechanism with pyridinium and form H adsorbates on the electrode surface through a one-electron PCET reaction. In contrast, the one-electron reduction to the imidazolium radical is predicted to occur at a much more negative potential (-2.63 V vs. SCE). These results are particularly valuable since they suggest that H adsorbates could be generated at low overpotentials by either of the two electrocatalysts. The H adsorbates might react as Pt-hydrides and reduce CO_2 through a proton coupled hydride transfer (PCHT) mechanism, as recently proposed for the electrocatalytic reduction of CO_2 to formic acid in the presence of pyridinium where the electrophilic attack of CO_2 onto the surface hydride is activated by the Brønsted acid in solution.

4 Supporting Information

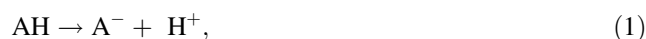
Supporting Information includes coordinates and thermodynamic data for the structural models reported in this paper as well as details on calculating $\text{p}K_a$ values for

weak acids in deuterated electrolyte. This material is available free of charge via the internet at <http://pubs.acs.org>.

Acknowledgements VSB acknowledges support from the AFOSR Grant# FA9550-13-1-0020 and supercomputing time from NERSC and from the high-performance computing facilities at Yale University. The authors thank M. Zahid Ertem for valuable discussions. ABB and KL acknowledges support from the Air Force Office of Scientific Research through the MURI program under AFOSR Award No. FA9550-10-1-0572 and the NSF under Award CHE-1308652.

Appendix

The reduction potential of the Brønsted acid ($\text{HA} = \text{PyrH}^+$, ImH^+) relative to the SHE, is obtained as the cell potential for the equilibrium:



which can be expressed as two half reactions:



and



The Gibbs free energy change ΔG for the overall reaction of Eq. (1) is given by

$$\Delta G = \Delta G^\circ + RT \ln \frac{[\text{A}^-][\text{H}^+]}{[\text{AH}]} \quad (4)$$

Which is essentially the Nernst equation upon substitution of $\Delta G^\circ = -F E^\circ$ and $\Delta G = -F E$:

$$E = E^\circ - (RT/F) \ln \frac{[\text{A}^-][\text{H}^+]}{[\text{AH}]} \quad (5)$$

At equilibrium, $\Delta G = 0$ and $[\text{A}^-][\text{H}^+]/[\text{AH}] = K_a$. Therefore,

$$E^0 = (RT/F) \ln K_{a(AH)} = -(RT/F \log e) \text{p}K_{a(AH)} \\ = -59 \text{ mV } \text{p}K_{a(AH)} \quad (6)$$

When $T = 298.15 \text{ K}$. Considering that $E^0 = E_{\text{PyrH}^+/\text{H(Pt)Pyr}}^0 - E_{\text{H}^+/\text{H(Pt)}}^0$, we obtain:

$$E_{\text{AH}/\text{H(Pt)A}^-}^0 = E_{\text{H}^+/\text{H(Pt)}}^0 - 59 \text{ mV } \text{p}K_{a(AH)} \quad (7)$$

References

- Kumar B, Llorente M, Froehlich J, Dang T, Sathrum A, Kubiak CP (2012) *Annu Rev Phys Chem* 63:541
- Benson EE, Sathrum AJ, Smieja JM, Kubiak CP (2009) *Chem Soc Rev* 38:89
- Costentin C, Robert M, Savéant J-M (2013) *Chem Soc Rev* 42:2423
- Barton CE, Lakkaraju PS, Rampulla DM, Morris AJ, Abelev E, Bocarsly AB (2010) *J Am Chem Soc* 132:11539
- Morris AJ, McGibbon RT, Bocarsly AB (2011) *ChemSusChem* 4:191
- Barton EE, Rampulla DM, Bocarsly AB (2008) *J Am Chem Soc* 130:6342
- Kamrath MZ, Relph RA, Johnson MA (2010) *J Am Chem Soc* 132:15508
- Boston DJ, Xu C, Armstrong DW, MacDonnell FM (2013) *J Am Chem Soc* 135:16252
- Yan Y, Zeitler EL, Gu J, Hu Y, Bocarsly AB (2013) *J Am Chem Soc* 135:14020
- Keith JA, Carter EA (2012) *J Am Chem Soc* 134:7580
- Keith JA, Carter EA (2013) *Chem Sci* 4:1490
- Lim C-H, Holder AM, Musgrave CB (2012) *J Am Chem Soc* 135:142
- Ertem MZ, Konezny SJ, Araujo CM, Batista VS (2013) *J Phys Chem Lett* 4:745
- Barrette WC, Johnson HW, Sawyer DT (1890) *Anal Chem* 1984:56
- Costentin C, Canales JC, Haddou B, Saveant J-M (2013) *J Am Chem Soc* 135:17671
- Canhoto C, Matos M, Rodrigues A, Geraldo MD, Bento MF (2004) *J Electroanal Chem* 570:63
- Peremans A, Tadjeddine A (1995) *J Chem Phys* 103:7197
- Tian Z-Q, Ren B (2004) *Annu Rev Phys Chem* 55:197
- Conway BE, Jerkiewicz G (2002) *Solid State Ionics* 150:93
- Ren B, Xu X, Li XQ, Cai WB, Tian ZQ (1999) *Surf Sci* 427–428:157
- Zolfaghari A, Chayer M, Jerkiewicz G (1997) *J Electrochem Soc* 144:3034
- Clavilier J, Armand D (1986) *J Electroanal Chem Interfacial Electrochem* 199:187
- Barber J, Morin S, Conway BE (1998) *J Electroanal Chem* 446:125
- Conway BE, Barber J, Morin S (1998) *Electrochim Acta* 44:1109
- Skulason E, Karlberg GS, Rossmeis J, Bligaard T, Greeley J, Jonsson H, Norskov JK (2007) *Phys Chem Chem Phys* 9:3241
- Skulason E, Tripkovic V, Bjorketun ME, Gudmundsdottir S, Karlberg G, Rossmeis J, Bligaard T, Jonsson H, Norskov JK (2010) *J Phys Chem C* 114:18182
- Nanbu N, Kitamura F, Ohsaka T, Tokuda K (2000) *J Electroanal Chem* 485:128
- Wiberg KB (1955) *Chem Rev* 55:713
- Oh Y, Hu X (2013) *Chem Soc Rev* 42:2253
- Morris AJ, Meyer GJ, Fujita E (1983) *Acc Chem Res* 2009:42
- Perdew JP, Burke K, Ernzerhof M (1996) *Phys Rev Lett* 77:3865
- Giannozzi P, Baroni S, Bonini N, Calandra M, Car R, Cavazzoni C, Ceresoli D, Chiarotti GL, Cococcioni M, Dabo I, Dal Corso A, de Gironcoli S, Fabris S, Fratesi G, Gebauer R, Gerstmann U, Gougoussis C, Kokalj A, Lazzeri M, Martin-Samos L, Marzari N, Mauri F, Mazzarello R, Paolini S, Pasquarello A, Paulatto L, Sbraccia C, Scandolo S, Sclauzero G, Seitsonen AP, Smogunov A, Umari P, Wentzcovitch RM (2009) *J Phys-Condens Matter* 21:395
- Dolg M, Wedig U, Stoll H, Preuss H (1987) *J Chem Phys* 86:866–872
- Hehre WJ, Radom L, Pvr Schleyer, Pople JA (1986) *Ab initio molecular orbital theory*. Wiley, New York
- Frisch MJ, Trucks GW, Schlegel HB, Scuseria GE, Robb MA, Cheeseman JR, Scalmani G, Barone V, Mennucci B, Petersson GA, Nakatsuji H, Caricato M, Li X, Hratchian HP, Izmaylov AF, Bloino J, Zheng G, Sonnenberg JL, Hada M, Ehara M, Toyota K, Fukuda R, Hasegawa J, Ishida M, Nakajima T, Honda Y, Kitao O, Nakai H, Vreven T, Montgomery JA, Peralta JE, Ogliaro F, Bearpark M, Heyd JJ, Brothers E, Kudin KN, Staroverov VN, Kobayashi R, Normand J, Raghavachari K, Rendell A, Burant JC, Iyengar SS, Tomasi J, Cossi M, Rega N, Millam JM, Klene M, Knox JE, Cross JB, Bakken V, Adamo C, Jaramillo J, Gomperts R, Stratmann RE, Yazyev O, Austin AJ, Cammi R, Pomelli C, Ochterski JW, Martin RL, Morokuma K, Zakrzewski VG, Voth GA, Salvador P, Dannenberg JJ, Dapprich S, Daniels AD, Farkas Ö, Foresman JB, Ortiz JV, Cioslowski J, Fox DJ (2010) *Gaussian 09, Revision A.02*; Gaussian, Inc.: Wallingford, CT
- Cramer CJ (2004) *Essentials of computational chemistry: theories and models*, 2nd edn. Wiley, Chichester
- Marenich AV, Cramer CJ, Truhlar DG (2009) *J Phy Chem B* 113:6378
- Bard AJ, Faulkner LR (2000) *Electrochemical methods: fundamentals and applications*, 2nd edn. John Wiley and Sons Inc., New York